ISSN 2229-5518

Synthesis and Characterization of In_2O_3 Nanomaterials

Gwen B. Castillon, Gil Nonato C. Santos

Abstract — Indium (III) Oxide (In_2O_3) nanomaterials were grown on glass and Si (100) substrates using the horizontal vapor phase crystal growth technique. A greater yield of nanomaterials was retrieved on the glass substrate than on the Si (100) substrate. Nanopyramids, nanooctahedrons, nanotriangles, and faceted nanoparticles were found at temperatures of 1200°C, 1000°C, and 800°C. EDX results of representative structures revealed an atomic composition of ~40% indium and ~60% oxygen. XRD results revealed that the nanomaterials produced were indeed indium oxide and that the sample grown on Si (100) has better crystallinity than those formed on glass. Transmission measurements confirm that the samples grown on the glass substrate were transparent to visible light with wavelengths of 528, 586, and 673 nm.

Index Terms— Indium (III) Oxide, Nanomaterials, Horizontal Vapor Phase Crystal Growth Technique

1 Introduction

In_2O_3 is an n-type semiconductor belonging to a special class of rare materials known as transparent conductive oxides (TCO) – materials with high optical transparency and high electronic conductivity at the same time. This type of materials has become essential components for optoelectronic applications and photoelectrochemical devices. The excellent carrier mobilities (>100cm^2/Vs) of In_2O_3 and its optical band gap outside the visible range (>3.2 eV) has been unmatched by other TCO's like ZnO and SnO_2 [1].

Among the applications of In_2O_3 nanomaterials is in the field of chemical sensing. In fact, several authors have studied its sensitivity to different materials like isopropene [3], nitrogen dioxide [2, 3], ethanol [2, 4, 5], ammonia [3, 4], benzene, toluene, LPG, 90 # gasoline, 97 # gasoline, and methane [4], hydrogen sulphide [6], ozone [7], and redox proteins, specifically, low density lipoprotein (LDL) and Cytochrome C [8].

The relatively low electron affinity (~3.5 eV), convenience of n-type doping, high chemical inertness, and sputter resistance of In_2O_3 also makes it one of the most attractive conductive oxides for field emission [9]. Also, because of its high refractive index of 2.0, 1D nanostructures of In_2O_3 are expected to function as waveguides for guiding and manipulating light on the micrometer scale [10].

In this study, the researcher attempted to grow In_2O_3 nanomaterials using a method developed in De La Salle University called Horizontal Vapor Phase Crystal Growth Technique. The said technique has successfully produced nanostructures of wurtzite (Zinc Oxide, ZnO) and rutile (Tin Oxide, SnO_2) crystal structures. This study is an attempt to produce nanostructures of In_2O_3 whose crystal structure is that of a body centered cubic crystal structure.

Unlike the other methods used in the synthesis of In_2O_3 nanomaterials by other researchers, the said method attempted to grow the nanomaterials in a sealed and evacuated glass tube instead of growing the nanomaterials in the presence of carrier gases. Also, no other catalysts or reagents were used x in the synthesis of In_2O_3 nanostructures. Synthesis was carried out a temperature of 800°C, 1000°C, and 1200°C while the growth time was set at 8 hours and the ramp time was set to 80 minutes.

- *Gwen B. Castillon, Master of Science in Physics, De La Salle University - Manila Philippines, E-mail: gwencastillon@yahoo.com*
- *Gil Nonato C. Santos, Doctor of Philosophy in Materials Science and Engineering, De La Salle University-Manila, Philippines. E-mail: santosg@dlsu.edu.ph*

2 Experimental Section

2.1 Synthesis of In_2O_3 Nanomaterials

Thirty-five milligrams of high purity In_2O_3 powder (99.99%) obtained from Aldrich Corporation was were loaded into a number of clean and dry closed-end glass tubes. Silicon subtrates were inserted into half of the closed end glass tubes. The closed-end glass tubes were then vacuum-sealed using a Thermionics High Vacuum System at a vacuum pressure of ~10^6 Torr. The vacuum-sealed glass tubes were then baked in a Thermolyne horizontal tube furnace. To achieve a temperature gradient necessary for the migration of the growth species and formation of the nanostructures, half of the length of a glass tube was allowed to protrude from the tube furnace. The morphology of the structures formed on the substrates were studied using a JEOL 5310 Scanning Electron Microscope, the elemental composition were determined using an Energy Dispersive X-ray Spectroscopy (Oxford with Link Isis), the crystal structure were verified using an XRD (Bede Scientific D3 System), and the optical transmission spectrum were taken using an Olympus BX61 upright fluorescence microscope.

ISSN 2229-5518

3 Results and Discussion

A. SEM Results

A 1-2 cm deposition band was found on the inner wall of the glass tubes as well as on the Si (100) substrate located a few centimeters from the heated end of the tube, particularly at the site were the temperature gradient existed.

Figure 1 shows the deposition bands formed on the inner wall of the glass tube as well as on the Si (100) substrate. It could be seen that the density of the nanomaterials in the deposition band on the Si (100) substrate is smaller than that of the density of nanomaterials in the deposition band on the glass wall. This is due to the fact that the flat surface of the Si (100) substrate has a much higher surface energy than the concave inner wall of the glass tubes [11].

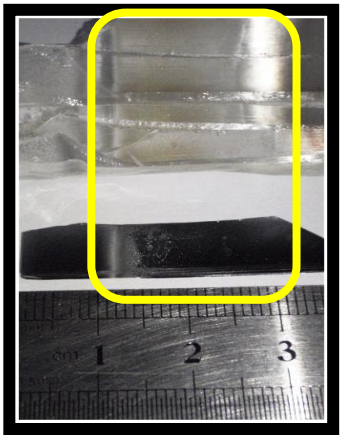

Fig. 1 Deposition band on Glass substrate and on Si(100) Substrate

Scanning electron microscopy revealed that micron sized crystals were formed on the left-most (hot) end of the deposition band, thin films were formed on the middle of the deposition band, while nanomaterials were formed on the right-most (cold) end of the deposition band.

Fig. 2 a, c, and e show the different structures formed on the glass substrate while Fig. 2 b, d, and f shows the structures formed on the Si (100) substrate at varying temperatures and at growth time of 8 hours. Pyramidal structures were the main structures formed at different temperatures on different substrates. Some octahedrons were found on the glass substrate at temperatures of 1200°C and 1000°C. Triangular nanostructures as well as faceteted nanoparticles were the dominant structures formed at a temperature of 800°C. Nanopyramids, nanooctahedrons, and nanotriangles having the (111) facets were frequently found because for a material with a cubic crystal structure like In_2O_3, the surface energy is considered to pursue the sequence $\gamma\{111\} < \gamma\{100\} < \gamma\{110\}$ [12].

The observation that octahedrons were consistently found at temperatures of 1000°C and 1200°C is consistent with Qurashi et. al.'s findings. The octahedrons were formed due to the high supersaturation ratio of In_2O_3 vapors at the deposition region that made the growth rates perpendicular to {111}, {100}, and {110} facets quite close [13].

The stuctures formed on the glass substrate were found to be smaller than that formed on the Si (100) substrate. This is possibly due to the lack of defect in the surface of the Si (100) substrate. There were no cracks or dents on the surface of the substrate that could have kept the nuclei from coalescing with other nuclei during the initial stage of the growth, and thus producing particles of dimensions in the micrometer scale.

It was also found that the size distribution was less uniform on the glass substrate than that on the Si (100) substrate. This could be due to the curvature of the glass tube as well as the rough surface of the unpolished glass wall that led to the uneven distribution of the growth species within the deposition region. On the other hand, the more uniform size distribution on the Si (100) substrate could be attributed to the flatness of its surface that allows a uniform distribution of the growth species along the surface of the Si (100) substrate.

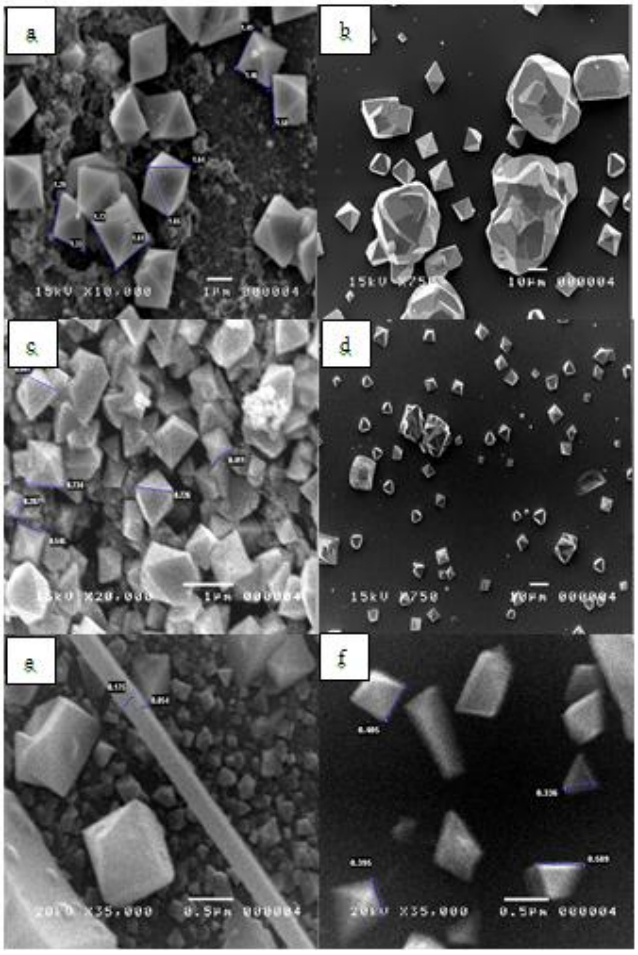

Fig. 2 (a) Octahedrons and pyramids with arrises lengths of ~1.4 -1.8 μm formed at 1200°C on glass, (b) pyramids, triangles, and faceted particles of lengths of ~1-100μm formed at 1200°C on Si (100), (c) Octahedrons and pyramids with arrises lengths of ~ 400-800 nm formed at 1000°C on glass, (d) pyramids, triangles, and faceted particles of lengths of ~3-40μm formed at 1000°C on Si (100), (e) pyramids, triangles, and faceted particles of lengths of ~50-900 nm formed at 800°C on glass, and (f) triangles, and faceted particles of lengths of ~300-600 nm formed at 800°C on Si (100)

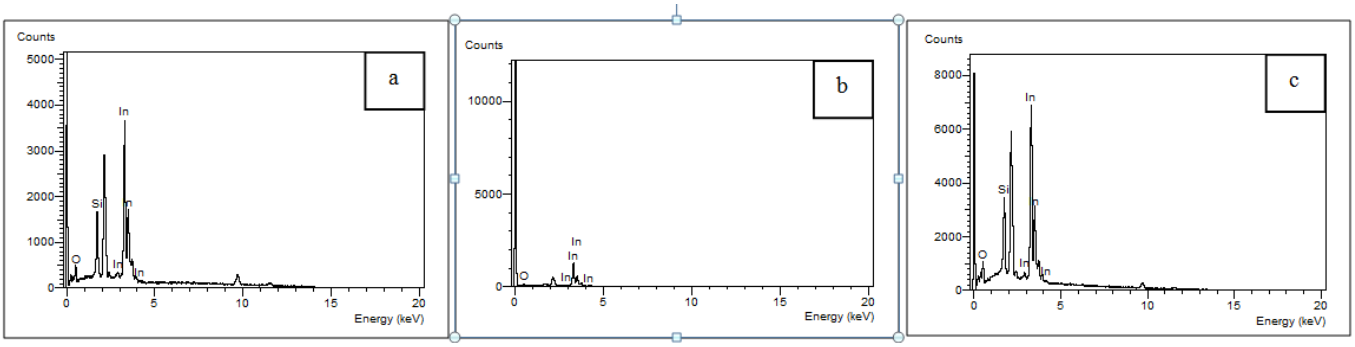

Fig. 3 EDX Spectrum of (a) a pyramid and (b) an octahedron formed at 1200°C, and (c) a triangle formed at 800°C

B. EDX Results

Fig. 3 a, b and c below are representative EDX spectra of an octahedron, a pyramid, and a triangle, respectively. The unlabeled peaks correspond to gold (Au), which was used in coating the samples for EDX characterization while the Si peaks are attributed to the glass substrate (SiO) or the Si (100) substrate.

Table 1 shows that the atomic ratios of Indium to Oxygen are ~41:59 for an octahedron, ~45:55 for a pyramid, and ~35:65 for a triangle. The said values are close to the theoretical value of the composition of In_2O_3 which is 40% indium and 60% oxygen. Similar results were found for other faceted particles although no discernable pattern was found regarding the effect of variation in growth temperature and substrate material.

TABLE 1. CALCULATED OXYGEN AND INDIUM CONTENT STRUCTURES

STRUCTURE	COMPOSITION (Atomic %)	
	Indium	Oxygen
Octahedron	41.12	58.88
Pyramid	45.31	54.69
Triangle	34.92	65.08

C. XRD Results

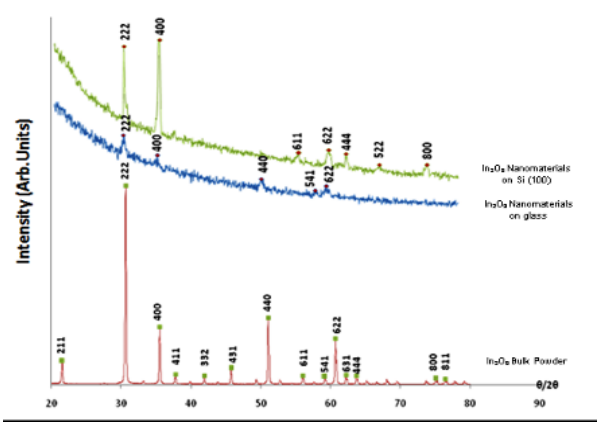

Fig. 4 X-ray Diffraction pattern of the bulk In_2O_3 powder and nanomaterials grown on glass and on Si (100) substrate at 800°C for 8 hours

The X-ray Diffraction pattern of the bulk In_2O_3 powder as well as the XRD pattern of the nanomaterials grown at a temperature 800°C and growth time of 8 hours on glass and on Si (100) is shown in the Fig. 4 below. The computed Miller indices of the lattice planes were found to be consistent with the standard values in literature for In_2O_3 with cubic c-type rare earth structure. [14]

The XRD patterns of the nanomaterials grown on glass and on silicon substrate were found to have similar XRD peaks with that of the XRD peaks of the source powder confirming the fact that the synthesized nanomaterials are indeed In_2O_3. The intensity of the prominent peaks at (222) and (400) for the nanomaterials grown at 800 °C and 8 hours on Si (100) substrate were found to be greater than the intensities of the same peaks for the samples grown at the same parameters on glass substrate.

Values of the lattice parameter *a* of In_2O_3 powder and that of In_2O_3 nanomaterials on glass and on Si (100) substrate were calculated from Bragg's Law and are shown on Table 2. The average Grain Sizes of the nanomaterials on glass and Si (100) are also shown in the table.

TABLE 2. LATTICE PARAMETER AND GRAIN SIZE OF In_2O_3 POWDER, In_2O_3 NANOMATERIALS ON GLASS, AND In_2O_3 ON SILICON

Sample	In_2O_3 powder	In_2O_3 on glass	In_2O_3 on silicon
Lattice parameter (nm)	1.0110	1.0192	1.0118
Grain Size (nm)	-	20.5895	41.1887

The values obtained were found to be consistent with the standard lattice parameter *a* for cubic In_2O_3 which is 1.0117nm [15]. The lattice parameter of the nanomaterials grown on Si (100) was found to be closer to the standard while the lattice parameter of the nanomaterials grown on glass was found to be greater than the standard. The average grain size, D, of the nanomaterials were calculated using Scherrer's Formula. It was found that the average grain size of the nanomaterials grown on Si (100) is greater than that of the nanomaterials grown on glass. This may be attributed to the reduction of the crystal defects originated from the structural similarity that the Si (100) have with In_2O_3 [28]. Both Si (100) and In_2O_3 have cubic structures.

The relatively high intensity of the diffraction peaks as well as the larger grain size of the samples grown on Si (100) substrate indicates that the sample grown on Si (100) had better crystallinity than that of the sample grown on glass.

D. Optical Characterization Results

Figure 5a below shows the spectrum of the light source used in the optical characterization of the samples. The source had peaks at 528, 586, and 673 nm. Figure 5b, on the other hand shows the transmission spectrum of the samples grown for 8 hours at a temperature of 1200°C (red), 1000°C (green), and 800°C (pink). It could be easily seen that the samples on glass were optically transparent to the wavelengths of the light source.

Optical characterization of the samples grown on the Si (100) substrate was not done, however, because the Si (100) substrate interferes with the transmission measurements.

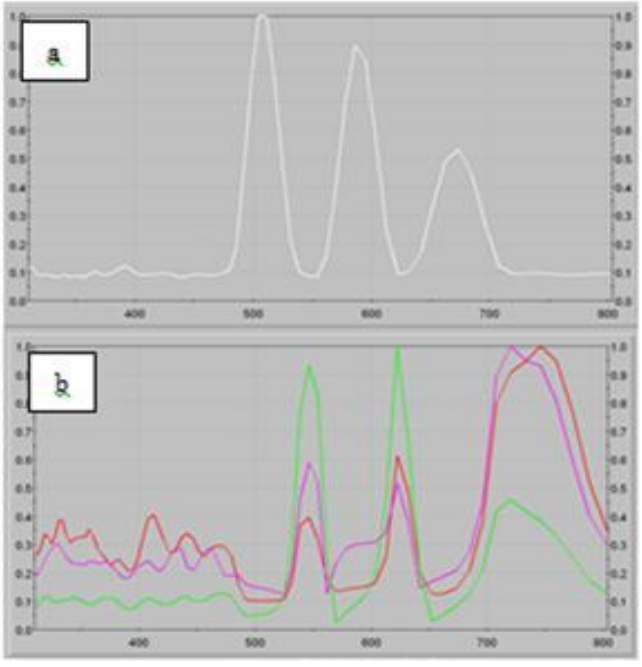

Fig. 5 Transmission spectrum of (a) the light source used for optical characterization and (b) transmission spectrum of In_2O_3 nanomaterials grown on glass – red for sample at 1200°C, Green for sample at 1000°C, and Pink for sample at 800°C

4 Conclusion

In_2O_3 nanomaterials were synthesized through the Horizontal Vapor Phase Crystal Growth deposition without a catalyst at a temperature of 1200°C, 1000°C, and 800°C and at growth times of 8 hours on Glass and on Silicon (100) Substrates.

SEM characterization revealed that the synthesized nanostructures had the morphology consistent to that of the cubic crystal structure: pyramidal, octahedral, and triangular.

It was observed that octahedrons were consistently found at temperatures of 1000°C and 1200°C. It was observed that there was little amount of nanostructures formed on the Si (100) substrate as compared to the amount of structures formed on glass. Also, the structures found on the Si (100) substrate were in the micrometer scale. The size distribution on the Si (100) substrate was also observed to be more uniform than that of the size distribution on the glass wall owing to the flat and uniform surface of the Si (100) substrate.

EDX characterization revealed that the structures had atomic compositions of ~40% indium and ~60% oxygen. XRD results revealed that the nanomaterials produced were indeed indium oxide and that the sample grown on Si (100) had better crystallinity than those formed on glass.

Optical characterization of the samples grown on glass substrate confirmed that the samples are transparent to visible light.

5 Acknowledgement

The aouthor would like to acknowledge the Department of Science and Technology-Science Education Institute for the financial aid and her advisers, Dr. Gil Nonato Santos and Dr. Reuben Quiroga for all the support

References

[1] A. Walsh, J. L. F.Da Silva, S-H. Wei, (17 November 2008). The SPIE website. [Online] Available: http://spie.org/x31451.xml?ArticleID=x31451

[2] S. Bianchi, E. Comini, M. Ferroni, G. Faglia, A. Vomiero, and G Sberveglieri, "Indium Oxide Quasi-Monodimensional Low Temperature Gas Sensor," *Sensors and Actuators B.*, vol. 118, pp. 204-207, 2006.

[3] C. Li, D. Zhang, S. Han, X. Liu, T. Tang, B. Lei, Z. Liu, and C. Zhou, "Synthesis, Electronic Properties, and Applications of Indium Oxide Nanowires," *Ann. N. Y. Acad. Sci.*, vol. 1006, pp. 104-103, 2003

[4] J. Xu, Y. Chen, and J. Shen, "Ethanol Sensor Based on Hexagonal Indium Oxide Nanorods Prepared by Solvothermal Method" *Materials Letters*, vol. 62, pp. 1363-1365, 2008.

[5] C. Xiangfeng, W. Caihong, J. Dongli, and Z.Chenmou, "Ethanol Sensor Based on Indium Oxide Nanowires Prepared by Carbothermal Reduction Reactions," *Chemical Physics Letters*, vol. 399, pp. 461-464, 2004.

[6] M. Kaur, N. Jain, K. Sharma, S. Bhattacharya, M. Roy, A. K. Tyagi, S. K. Gupta, and J. V. Yakhmi, "Room-temperature H_2S Gas Sensing at pbb Level by Single Crystal In_2O_3 Whiskers," *Sensors and Actuators B*, vol. 133, pp. 456-461, 2008.

[7] G. Sberveglieri, C. Barrato, E. Comini, G. Faglia, M. Ferroni, A. Ponzini, and A. Vomiero, "Synthesis and Characterization of Semiconducting Nanowires for Gas Sensing" *Sensors and Actuators B.*, vol. 121, pp. 208-213, 2007.

[8] M. Rouhanizadeh, T. Tung, C. Li, G. Soundararajan, C. Zhou and T. Hsiai The IEEE website. [Online] Available: http://ieeexplore.ieee.org/stamp/stamp.jsp?arnumber=01290615.

[9] Q. Wang, K. Yu, F. Xu, J. Wu, Y. Xu, and Z. Zhu, "Synthesis and Field Emission Properties of In_2O_3 Nanostructures," *Materials Letter*, vol. 62, pp. 2710-2713, 2008.

[10] T. Tsuruoka, C. H. Liang, K. Terabe, and T. Hasegawa, "Optical Waveguide Properties of Single Indium Oxide Nanofibers," *Journal of Optics A*, vol. 10, 0550201 (5pp), 2008.

[11] G. Cao, and S. Limmer, "Oxide Nanowires and Nanorods" In H. S. Nalwa (Ed.), *Encyclopedia of Nanoscience and Nanotechnology*, pp. 377-396, Calif.: American Scientific Publishers, 2004.

[12] A. Qurashi, E. M. El-Maghraby, T. Yamazaki, Y. Shen, and T. A Kikuta, "Generic Approach for Controlled Synthesis of In_2O_3 Nanostructures for gas sensing applications," *Journal of Alloys and Compounds*, vol. 481, pp. L35 – L39, 2009.

[13] A. Qurashi, E. M. El-Maghraby, T. Yamazaki, and T. A Kikuta, "Catalyst-free Shape Controlled Synthesis of In_2O_3 Pyramids and Octahedron: Structural Properties and Growth Mechanism," *Journal of Alloys and Compounds*, doi: 10.1016/j.jallcom.2009.01.112, 2008.

[14] M. Girtan, G. I. Rusu, G. G. Rusu, and S. Gurlui, "Influence of Oxidation Conditions on the Properties of In_2O_3 Films," *Applied Surface Science*, pp. vol. 162-163, 492-498. (2000).

[15] D. Calestani, M. Zha, A. Zappettini, L. Lazzarini, and L. Zanotti, "In-catalyzed Growth of high Purity Indium Oxide Nanowires," *Chemical Physics Letters*, vol. 445, pp. 251-254, 2007

[16] J.-B. Lee, M.-H. Lee, C.-K. Park, and J.-S. Park, "Effects of Lattice Mismatches in ZnO/substrate Structures on the Orientations of ZnO Films and Characteristics of SAW Devices," *Thin Solid Films*, vol. 447-448, pp. 296-301, pp. 2004.